encit 2022

ABCM Associação Brasileira de Engenharia e Ciências Mecânicas

19th Brazilian Congress of Thermal Sciences and Engineering
November 6th–10th, 2022, Bento Gonçalves - RS - Brazil

ENC-2022-0194
GUIDELINES ON THE USAGE OF SYSTEM IDENTIFICATION TECHNIQUES IN AEROELASTIC STUDIES

Marcus Vinicius Gama Muniz
Instituto Tecnológico de Aeronáutica (ITA) - Praça Marechal Eduardo Gomes, 50 - 12298-900 - São José dos Campos - SP - Brazil
marcusvgmuniz@gmail.com

João Luiz F. Azevedo
Instituto de Aeronáutica e Espaço (IAE) - Praça Marechal Eduardo Gomes, 50 - 12298-904 - São José dos Campos - SP - Brazil
joaoluiz.azevedo@gmail.com

Abstract. *The present work employs linear system identification techniques, SISO and MIMO algorithms, to the identification of aerodynamic loads over a NACA 0012 airfoil subject to an unsteady airflow. The aerodynamic response of the aeroelastic system to different inputs in both pitch and plunge degrees of freedom are computed by numerically solving the unsteady Euler equations. Three different types of excitations are used in the study of the SISO methodology: exponential pulse, discrete step and unit sample. The strengths and drawbacks of each of these inputs are exposed alongside a discussion on how the interpretation of the CFD solver as a discrete-time system impacts some of the CFD solver parameter settings. The more efficient MIMO methodology is employed using Walsh functions as the excitations of the airfoil degrees of freedom. The power spectral density (PSD) and cross-power spectral density (CPSD) functions, between the inputs and outputs, are computed using the Welch algorithm to obtain the aerodynamic transfer functions of the responses in lift and moment coefficients due to both pitch and plunge inputs. Additional requirements are set to the shape of Walsh functions and also to the Discrete Fourier Transform windows leading to a more precise identification process. A flutter stability analysis is also performed to compare each of those algorithms.*

Keywords: *Flutter Prediction, System Identification, Computational Fluid Dynamics, CFD*

1. INTRODUCTION

The study of the application of linear time invariant (LTI) systems theory in the context to the aeroelastic analysis in the research group at Instituto de Aeronáutica e Espaço (IAE) traces back to the work of Oliveira (1993) inspired by Rausch *et al.* (1990). In that work, the two-dimensional Euler equations of fluid mechanics were solved using a finite volume method and the aerodynamic transfer function of the lift force and pitch moment coefficients were identified using a Single Input-Single Output (SISO) approach following the work of Vepa (1977). It also demonstrates the efficiency gain provided by the use of these techniques to the analysis of a huge number of values for the aeroelastic parameters such as air speed, inertia and stiffness of the aeroelastic system. However, due to the computational limitation back then it was not possible a complete assessment of all the capabilities of the methodology, task that would require studies considering variation of parameters relevant to the simulation such as pulse duration, displacement amplitude, among others. Marques and Azevedo (2008a) performed these studies and also demonstrated that, although the Euler equations are nonlinear, for small disturbances in the pitch and plunge displacements, the theory of linear systems could be applied using the state space formulation for the equations of motion of the aeroelastic system. Azevedo *et al.* (2012) extended these studies applying a Multiple Input-Multiple Output (MIMO) approach to the same aeroelastic system previously studied requiring a unique unsteady CFD run to obtain all data necessary to the identification process, following the work of Raveh (2001), Raveh (2004) and Kim *et al.* (2005). This is in contrast to one CFD run per degree of freedom, required by the SISO approach. Although that work demonstrated the efficiency of this approach, it also indicated that there were some robustness issues in the overall system identification process that would require further analyses. In other words, for some of the cases analyzed, the methodology worked very well, while for others the results were rather oscillatory or inaccurate.

The present work revisits some of the issues previously indicated. It also presents further discussion of the consequences of the different interpretations presented by Marques and Azevedo (2008b) of the CFD solver as a discrete time

system, rather then the usual interpretation of a mere approximation of a continuous time system. Additionally, a study of the results obtained by Azevedo *et al.* (2013) is presented explaining the reasons for the successful results of some cases, while not for all cases analyzed in that reference. To conclude, the authors gathered the experience obtained on those previous efforts, together with the outcome of the present study, in order to devise some guidelines that help improve the aeroelastic system identification process and, therefore, lead to well-identified aerodynamic transfer functions.

2. THEORETICAL FORMULATION

2.1 Basic Aeroelastic Formulation

In this work, an aeroelastic analysis is performed on a wing typical section modeled as a two-dimensional NACA 0012 aerodynamic profile as illustrated in Fig. 1. Two degrees of freedom are used to describe the movement of the typical section, its angular displacement in pitch and linear displacement in plunge, respectively represented as α and h in that figure.

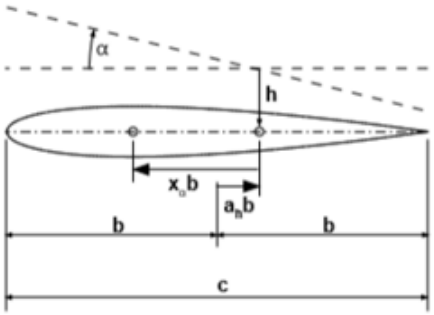

Figure 1. Wing typical section.

The equation modeling the aeroelastic system is given by

$$[M]\{\ddot{\eta}(t)\} + [K]\{\eta(t)\} = Qa(t), \tag{1}$$

where:

$$\{\eta\} = \begin{bmatrix} \xi(t) \\ \alpha(t) \end{bmatrix}, \tag{2}$$

is the vector containing the non dimensional generalized coordinates describing the displacements in both pitch (α) and plunge (ξ) degrees of freedom. The generalized coordinate describing the displacement in plunge, ξ, is obtained by dividing the physical coordinate, h, by the typical section semi chord b, $\xi = h/b$.

$$[M] = \begin{bmatrix} 1 & \chi_\alpha \\ \chi_\alpha & r_\alpha^2 \end{bmatrix}, \tag{3}$$

is the generalized dimensionless mass matrix. This matrix is described in terms of the dimensionless static unbalance, χ_α, and the dimensionless radius of gyration, r_α. The dimensionless static unbalance is given by $\chi_\alpha = S_\alpha/mb$. $S_\alpha = mx_ab$ is the dimensional static unbalance function of m the mass of the airfoil, x_a the distance of the elastic axis to center of mass, and b the semi chord as shown if Fig 1. The dimensionless radius of gyration is given by, $r_\alpha = \sqrt{I_\alpha/mb^2}$, where I_α is moment of inertia measured on the pitch axis passing through the center of mass.

$$[K] = \begin{bmatrix} \omega_h & 0 \\ 0 & r_\alpha^2\omega_\alpha^2 \end{bmatrix}, \tag{4}$$

is the generalized stiffness matrix described in terms of the natural circular frequencies for the plunge and pitch modes, $\omega_h = \sqrt{k_h/m}$ and $\omega_\alpha = \sqrt{k_\alpha/I_\alpha}$, respectively. k_h is the stiffness of the typical section in the plunge structural mode and k_α is the stiffness in the pitch structural mode. The vector containing the aerodynamic loads, i.e, lift force and pitch moment, is given by

$$\{Qa(t)\} = \begin{bmatrix} \frac{Qa_h(t)}{mb} \\ \frac{Qa_\alpha(t)}{mb^2} \end{bmatrix} . \tag{5}$$

The above equations are dimensionless in terms of the generalized displacements, however not in the time. In order to make them non dimensional also in terms of the time variable a reference circular frequency, ω_r, which will be termed ω_α herein, is used to obtain the non dimensional time variable $\overline{t} = t\omega_r$. Using the chain rule for time derivatives, one obtains the non dimensional form of the equation of motion, Eq. 1, as:

$$[M]\{\ddot{\eta}(\overline{t})\} + [\overline{K}]\{\eta(\overline{t})\} = \{\overline{Qa}(\overline{t})\}, \tag{6}$$

The generalized mass matrix, $[M]$, is the same as previously described in Eq. 3 as none of its terms is dependent on time whereas

$$[\overline{K}] = 1/\omega_r^2[K] \tag{7}$$

and

$$\{\overline{Qa}(\overline{t})\} = 1/\omega_r^2\{Qa(\overline{t})\}. \tag{8}$$

The aerodynamic lift force and pitch moment are obtained using the fluid mechanics Euler equations solved by a CFD code developed in the research group. Marques and Azevedo (2008a) shows that, under the assumption of small perturbations, a linear relation between the unsteady aerodynamic forces and moments and the displacements in pitch and plunge can be assumed even at high Mach numbers, where the Euler equations have a strong nonlinear character. This context warrants the use of the well-developed linear time invariant (LTI) system theory to predict and simulate the behavior of the aeroelastic system represented by the typical section by the convolution operation. This operation defined in the time domain by a cumbersome integral, Eq. 11, is more easily performed in the frequency domain where it turns out to be a simple multiplication operation. In the frequency domain, the equations of motion, Eq. 2, are given by

$$\overline{s}^2[M]\{\ddot{\chi}(\overline{s})\} + [\overline{K}]\{\chi(\overline{s})\} = \overline{Qa}(\overline{s}), \tag{9}$$

where $\overline{s} = s/\omega_r$, is the non dimensional Laplace transform variable; $\chi(\overline{s})$, is the Laplace transform of the generalized coordinate vector; and $\overline{Qa}(\overline{s})$is the Laplace transform of the aerodynamic load vector given by the following relation, using the linear assumption,

$$\overline{Qa}(\overline{t}) = \frac{(U^*)^2}{\pi\mu}[A(\overline{s})]\{\eta(\overline{s})\}, \tag{10}$$

where $\mu = m/(\pi\rho_\infty b^2)$ is the system mass ratio, $U^* = U_\infty/(b\omega_r)$ is the characteristic speed, and $A(\overline{s})$ is the aerodynamic load transfer function whose identification is the essence of the effort described in the present work.

2.2 Identification of Aerodynamic Transfer Functions

Linear continuous time invariant (LTI) systems have the property that the response to impulsive excitations contains all information about the system and the response to every other input is obtained by the convolution integral, Isermann and Munchhof (2009):

$$y(t) = h(t) * x(t) = \int_0^t G(\lambda)x(t-\lambda)d\lambda \tag{11}$$

where $G(\lambda)$ is the transfer function of the system. As the unit impulse is the derivative of the step function, it can be shown that the transfer function can also be obtained applying a step excitation to the system. In face of the infeseability of numerical implementation of the theoretical continuous time impulse and indicial (step) excitations, the general approach to the problem is the use of smooth pulse excitations, more specifically the exponential pulse (EP) shown in Fig. 2, which can be given by

$$f_p(t) = \begin{cases} 4\left(\frac{t}{t_{max}}\right)^2 exp\left(2 - \frac{1}{1-\frac{t}{t_{max}}}\right), 0 \leq t < t_{max} \\ 0, t \geq t_{max} \end{cases} \tag{12}$$

The usual thinking of analyzing aerodynamic systems as continuous-time systems leads to the interpretation of this function as a mere approximation to the unit impulse excitation in a continuous system. However, this is a wrong approach and discrete systems have an exact representation for the unit impulse, which is the unit sample (Marques and Azevedo, 2007, 2008a). Hence, the use of time-discretized versions of the smooth pulse excitations is, actually, a discrete time approximation of the unit sample. This approximation leads to missing the information of the system for a wide frequency range, preventing an adequate prediction of the system transfer function. Depending on the analysis being carried out, this is not a true issue, as will be shown later in this work. However, as explained by Marques and Azevedo (2007) and Silva

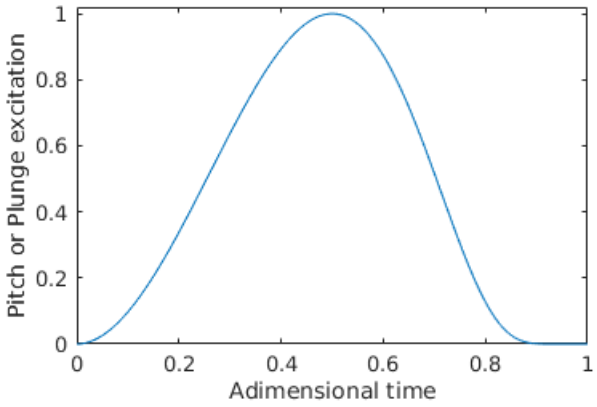

Figure 2. Exponential Pulse Excitation.

(1997), the usage of equivalent discrete-time excitations, such as the unit sample or the discrete step, is a better approach as they are capable of exciting the entire system frequency range. Marques and Azevedo (2007) show that the transfer function of the aerodynamic system can be obtained from the response to a unit sample (US) or discrete step inputs (DS), defined as

$$\delta[n] = \begin{cases} 0, n \neq 0, \\ 1, n = 0, \end{cases} \tag{13}$$

and

$$u[n] = \begin{cases} 0, n \leq 0, \\ 1, n > 0. \end{cases} \tag{14}$$

For discrete time systems, the transfer functions, $h[n]$, are the response of the system to the unit sample input

$$G[n] = S_{US}[n] \, . \tag{15}$$

The discrete step function can also be used to excite the system and the transfer function is obtained by

$$G[n] = S_{DS}[n] - S_{DS}[n-1] \, . \tag{16}$$

Marques and Azevedo (2007) also remark that the unit sample cannot be confused with a sampled version of a triangular continuous-time function. Whereas for continuous-time triangular functions reducing the sampling time (δt) uncovers previously hidden data in the signal, even for infinitesimal values of δt, the same does not happen for discrete-time system since there is no information at sampling times smaller than the system characteristic time step. One subtle, however important, difference that the discrete system interpretation brings to the subject is that the time step used in the CFD solution does not have any impact capturing the whole frequency content of the system. The difference in the resultant transfer functions, for different non dimensional time steps, if exists, should be credit to the capability to correct solve the airflow by the CFD solver with the two different parameters, and never to a difference in the frequency content being resolved by each of those runs, as they are absolutely the same, as previously stated. Another difference brought by this interpretation is related to the transfer function obtained by the response to the discrete step input. The discrete LTI system view of the problem leads to the calculation of the transfer function by Eq. 16. The wrong interpretation of the system as a continuous time system would lead one to view this equation as a ratio of the time derivatives output and the input of the system, what is clearly wrong as there is no reference to the time step in its denominator.

The transfer functions using the MIMO approach are obtained from the power spectral density (PSD) and cross-power spectral density (CPSD) functions, Isermann and Munchhof (2009), by

$$G_{ij} = \frac{S_{inp_i out_j}}{S_{inp_i}} \, , \tag{17}$$

where S_{inp_i} is the PSD of the input signal "i" and $S_{inp_i out_j}$ is the CPSD of the output signal "j" an the input signal "i" These functions are the application of the Fourier transform to the auto-correlation and cross-correlation functions for one or two different signals given by:

$$R_{xy} = \lim_{T \to \infty} \int_{-\frac{T}{2}}^{\frac{T}{2}} x(t) y(t-\tau) dt, \tag{18}$$

where the auto-correlation function is obtained when $x(t) = y(t)$ whereas the cross-correlation is obtained for $x(t) \neq y(t)$.

The Fourier transform theory is constructed based on the assumption of an infinite periodic function. When applied to discrete systems by the use of the DFT, the input signal can be seen as the multiplication of an infinite periodic function by a sampling function, known as a window function. Figure 3 shows this process for a sinusoidal function with no loss of generality. More on the discussion of the windowing process can be seen in Harris (1978). To improve the quality of the system identification the Welch algorithm (Welch, 1967) was employed to obtain the PSD and CPSD functions. This algorithm segments signals in a predefined number of sections and apply windows with predefined shapes computing the DFT to each of these segments. The resultant spectral density functions are the average of the DFT of all these sections. In his work, Azevedo (2013) applied several combinations of distinct excitation functions and window parameters in order to obtain the transfer functions of the aeroelastic system. Some of those combinations resulted in very good approximations of the system transfer functions, whereas for others the results were incorrect. The present authors studied the different responses to different window settings and could understand those different results, finally proposing some guidelines that lead to the accurate calculation of the expected results.

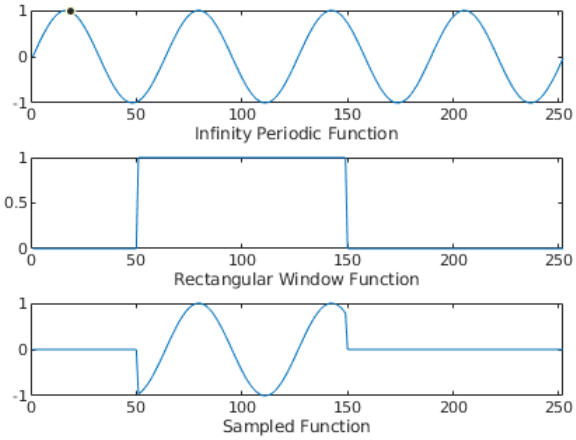

Figure 3. Sampling process: window definition.

The next step in the aeroelastic analysis, after the proper transfer function identification, either by the SISO or MIMO approaches, is to cast them in an appropriate form to be used in a state-space formulation and, then, proceed to the root-locus analysis in order to assess the stability of the system. One appropriate form is the well-known Rational Function Approximation (RFA), more specifically the first form of the Eversman and Tewari polynomials (Eversman and Tewari, 1991), given by

$$[A(\overline{\overline{s}})] = [A_0] + [A_1]\overline{\overline{s}} + [A_2]\overline{\overline{s}}^2 + \sum_{n=1}^{n_\beta} \left([A_{n+2}] \frac{1}{\overline{\overline{s}} + \beta_n} \right), \tag{19}$$

where n_β is the number of poles in the rational function, β_n are the poles in the rational function, which introduce the aerodynamic lags with respect to the structural modes, and ($\overline{\overline{s}} = sb/U_\infty$ is the complex Laplace variable in dimensionless form. The coefficients of the rational polynomial (A_i), the number of poles and the poles themselves are obtained by an optimized least-squares approximation method in which the nonlinear lag parameters (β_n) are interactively evaluated with a Simplex Search Method (Lagarias *et al.*, 1998).

2.3 Flutter Stability Analysis

The final step to establish the flutter boundaries is the root locus analysis. Such an analysis is performed by solving the eigenvalue problem for each value of the U^* parameter, that is,

$$([D] - \overline{s}[I_{NXN}])\{\chi(\overline{(s)})\} = \{0_{NX1}\}, \tag{20}$$

where $[D]$ is the stability matrix and $N = 2n_\beta + 4$. The stability matrix is obtained after casting the aeroelastic equations of motion, Eq. 2, in the state space form. Applying the RFA proposed in Eq. 19 to Eq. 6, the stability matrix is given by

$$[D] = \begin{bmatrix} [D_{\eta\eta}] & [D_{\eta\alpha}] \\ [D_{\alpha\eta}] & [D_{\alpha\alpha}] \end{bmatrix}, \tag{21}$$

where

$$[D_{\eta\eta}] = \begin{bmatrix} -[\mathbf{M}]^{-1}[\mathbf{C}] & -[\mathbf{M}]^{-1}[\mathbf{K}] \\ I_{2x2} & 0_{2x2} \end{bmatrix}, \tag{22}$$

$$[D_{\eta\alpha}] = \begin{bmatrix} \frac{(U^*)^3}{\pi\mu}[\mathbf{A_3}] & \frac{(U^*)^3}{\pi\mu}[\mathbf{A_4}] & \dots & \frac{(U^*)^3}{\pi\mu}[\mathbf{A_{n_\beta+2}}] \\ [0_{2x2}] & [0_{2x2}] & \dots & [0_{2x2}] \end{bmatrix}, \tag{23}$$

$$[D_{\alpha\eta}] = \begin{bmatrix} [0_{2x2}] & [I_{2x2}] \\ [0_{2x2}] & [I_{2x2}] \\ \dots & \dots \\ [0_{2x2}] & [I_{2x2}] \end{bmatrix}, \tag{24}$$

$$[D_{\alpha\alpha}] = \begin{bmatrix} -U^*\beta_1[I_{2x2}] & [0_{2x2}] & \dots & [0_{2x2}] \\ [0_{2x2}] & -U^*\beta_2[I_{2x2}] & \dots & [0_{2x2}] \\ \dots & \dots. & \dots & \dots \\ [0_{2x2}] & [0_{2x2}] & \dots & -U^*\beta_n[I_{2x2}] \end{bmatrix}, \tag{25}$$

$[\mathbf{A_n}] = [M]^{-1}[A_n]$, $[\mathbf{M}] = [M] - 1/(\pi\mu)[\mathbf{A_2}]$, $[\mathbf{K}] = [\overline{K}] - (U^*)^2/(\pi\mu)[\mathbf{A_0}]$, and $[\mathbf{C}] = -(U^*)/(\pi\mu)[\mathbf{A_1}]$.

3. RESULTS

3.1 Single Input–Single Output (SISO) System Identification Techniques

In the present analyses, the flow around an airfoil at Mach number 0.8 is simulated for three different inputs in its pitch and plunge displacements: exponential pulse, discrete step and unit sample. The amplitudes considered for the exponential pulse perturbations are 0.001° and 0.0001c, where c is the reference chord, respectively, while, for the discrete step and unit sample inputs, the amplitudes are 0.0001° and 0.000001c. Except otherwise stated, the time step of the simulations is 0.003 non-dimensional time units and a total of 300 time units are simulated. Figure 4 shows the mesh used for the present study.

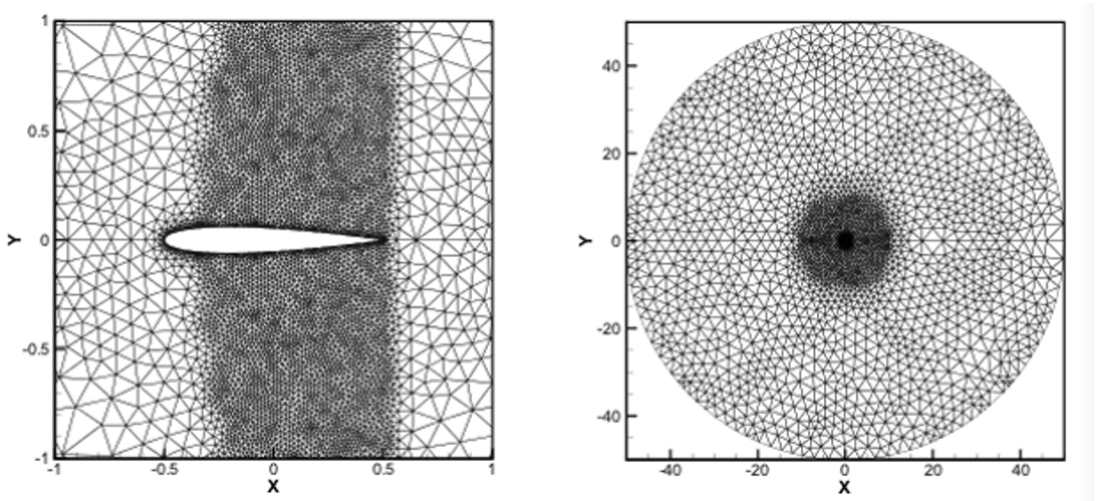

(a) Mesh detail around airfoil. (b) Complete mesh.

Figure 4. NACA 0012 Airfoil Mesh

The first analysis is on the transfer functions obtained by a perturbation in both pitch and plunge degrees of freedom in the form of the exponential pulse previously described by Eq. 12 using a pulse with duration (t_{max}) of 1 non dimensional time unit. The duration of the pulse impacts on the frequency content that is actually excited in the solution as only the theoretical pulse, or step functions, are capable to excite the entire frequency range. So, the pulse duration may limit the quality of the identification procedure for higher frequencies. In order to understand the sensitiveness of the frequency content range to the length of the pulse the transfer functions were obtained exciting the system using the following values of t_{max}: 5, 10 and 50. Each of those exponential pulses are shown in Fig. 5 The transfer functions obtained for each of the pulse lengths are shown in Fig. 6. As expected for higher frequencies the frequency content of the transfers functions become different. This is evidenced in the $G_{C_L,\alpha}$ plot where both transfer functions visually match for 5 and 10 time units whereas for 50 time units the real part turns different for reduced frequency $1 < k < 3$.

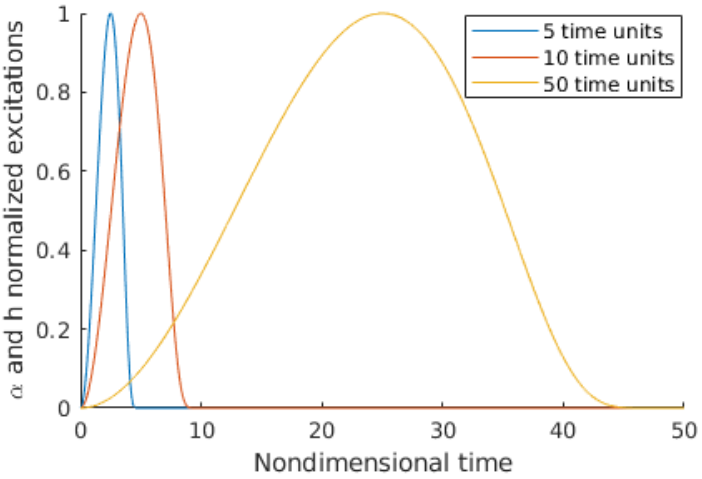

Figure 5. Exponential pulse excitation with varying lengths.

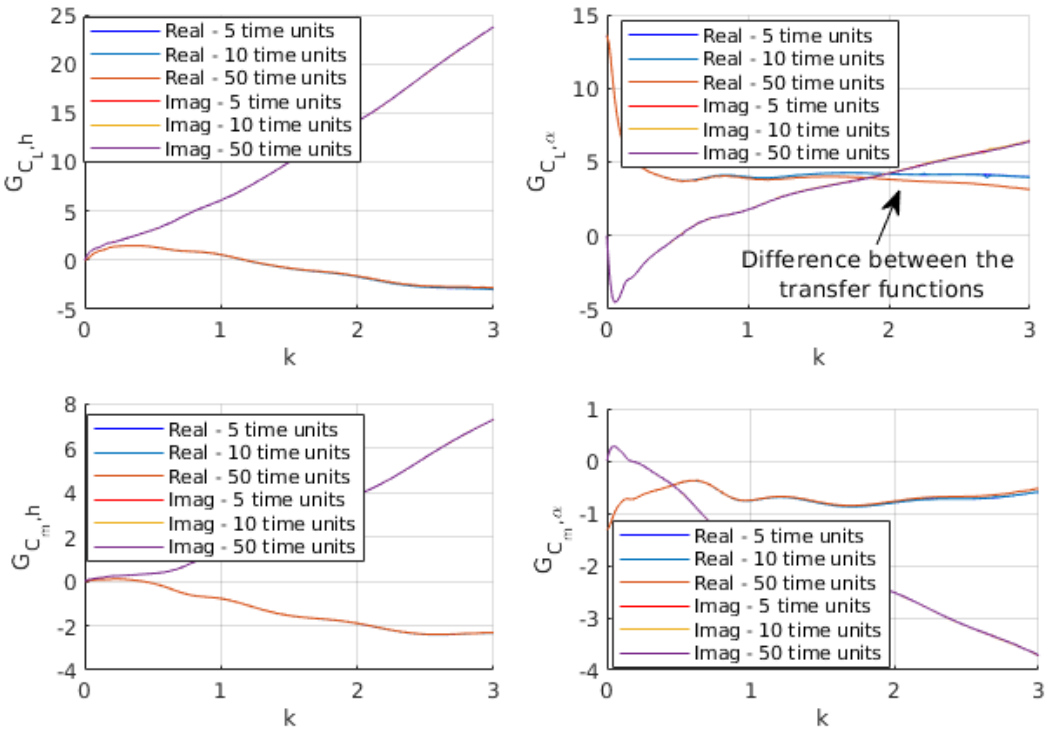

Figure 6. Transfer functions obtained from varying exponential pulse length.

As previously discussed, Silva (1997) suggested the use of discrete step and unit sample sequences to excite the system. Figure 7 shows a comparison of the transfer functions obtained with both exponential pulse, with duration of 1 non dimensional time unit, and discrete step pulse. The transfer functions obtained with both excitations have a good agreement except for very low reduced frequencies, as show in the rightmost part of the figure, in the detail of the $G_{C_L,\alpha}$ transfer function.

Marques and Azevedo (2008a) show that it is possible, with the rigid mesh displacement formulation, to obtain the same transfer functions using both the DS and US inputs. However, this was only true due to the extremely small perturbations used to excite each structural mode. In the present work, and using perturbations which are larger that those employed in Marques and Azevedo (2008a), it was not possible to reproduce the same results when using the US input. Figure 8 presents the time histories obtained herein for the aerodynamic coefficients calculated from an US excitation in both pitch and plunge degrees of freedom, as well as the differential coefficients at each time step resulting from a DS excitation , which are the actual data used to obtain the transfer functions for this excitation, as shown in Eq. 16. There is no discernible difference between these data in the time domain leading to the wrong conclusion that the same transfer functions can be obtained from both approaches as they are just the application of the Fourier transform to this data. The

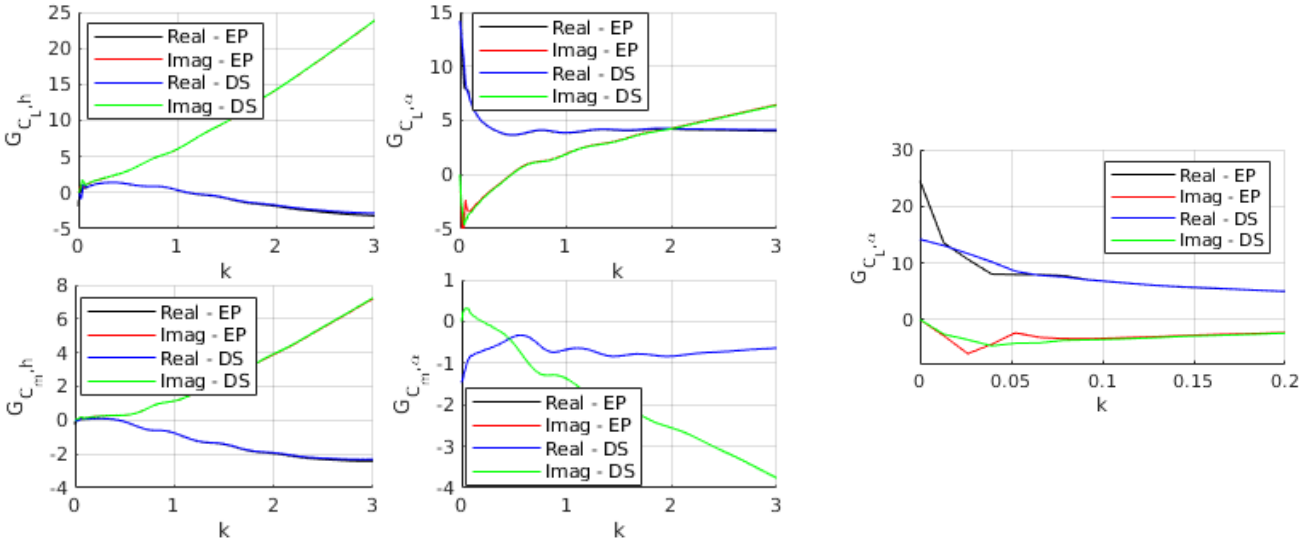

Figure 7. Transfer functions resulting from EP and DS excitations.

actual differences between the US and DS data are presented in Fig. 9, which are of order of 10^{-6} in magnitude for the lift and moment coefficients, due to the pitch input, whereas for the plunge input the difference is "zero", to machine accuracy.

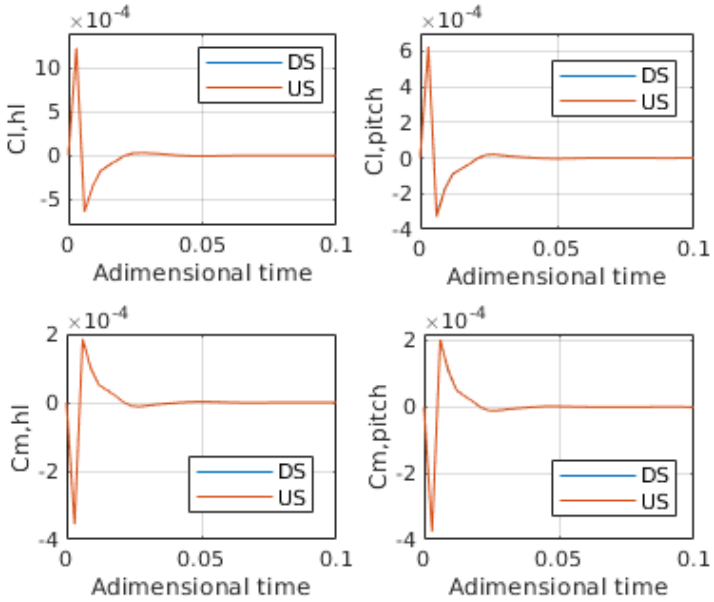

Figure 8. DS and US time domain data used in the system identification equations.

One may argue that those differences are negligible in the context of an aeroelastic analysis. However, the whole picture becomes clearer when the transfer functions are analyzed. Figure 10 shows that, for the plunge transfer functions, the results from either discrete step or unit sample can be used, as expected since their differences are of the order of machine accuracy. On the other hand, for the pitch input, the resulting transfer functions are only reasonable when using the discrete step functions. This analysis shows that the discrete step approach is more robust to errors in the CFD calculations and also to numerical limitations of the hardware used. The reasons for the differences in the US results are most certainly associated to the fact that the unit sample perturbation is more aggressive than the discrete stp one, for the same amplitude. Hence, the CFD solver can cope with the DS perturbation, whereas it may not be able to do so for the unit sample, again, for the same level of perturbation. Hence, although Marques and Azevedo (2008a) show that, from an analytical standpoint, both the discrete step and unit sample are equivalent approaches, the present work is demonstrating that, from a numerical perspective, the use of the DS input yields a more robust behavior. Therefore, it should be preferred approach. For completeness, it must be mentioned that the work of Marques and Azevedo (2008a) already indicated such conclusion, although without the actual results demonstrating the possible errors arising from the use of the unit sample perturbation, as done in the present work.

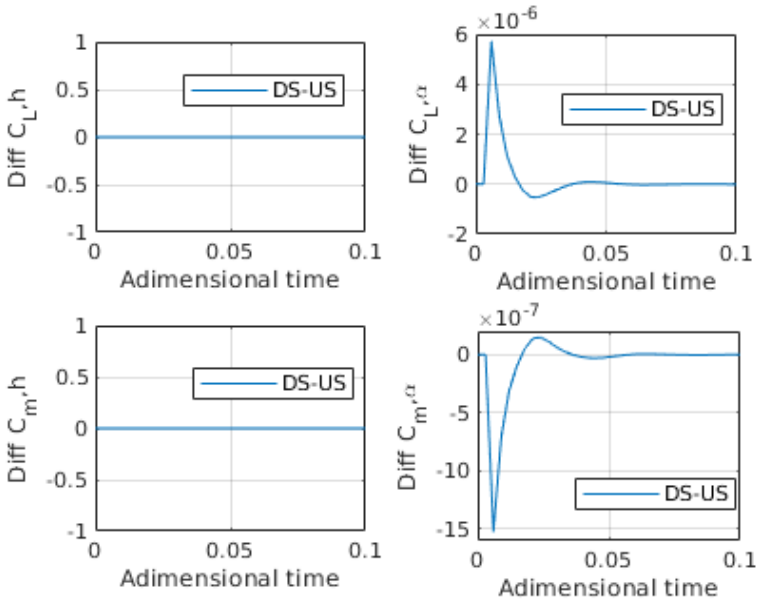

Figure 9. Differences on the data obtained from DS and US excitations.

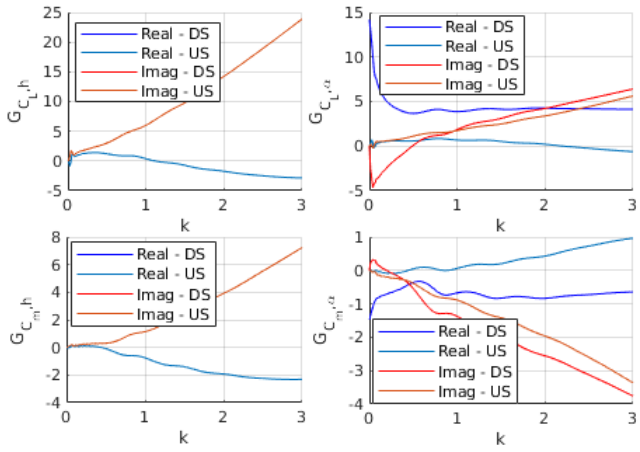

Figure 10. Transfer functions obtained from DS and US excitations.

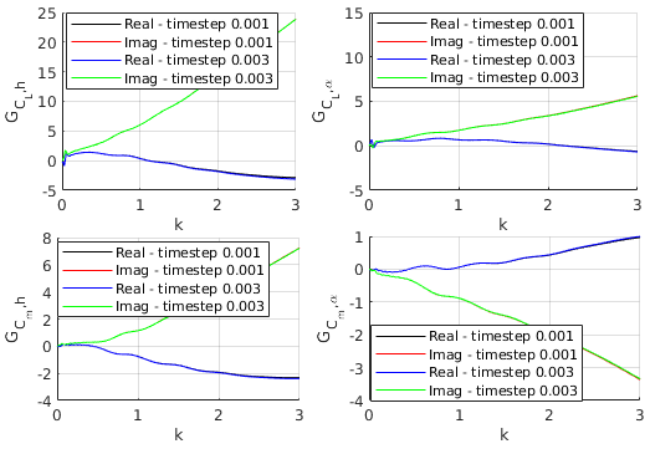

Figure 11. Aerodynamic transfer functions from US excitations with different timesteps.

Figure 11 shows de transfer functions for a NACA 0012 airfoil at a free stream flow with Mach number 0.8, subject to two US inputs in the pitch and plunge degrees of freedom, but using different integration time steps in each computation. One calculations uses a time step of 0.001 dimensionless time units while the other uses a time step of 0.003 dimensionless time units. The total non dimensional time of the simulation is the same, 300 dimensionless time units. It is clear that the transfer functions match each other. As previously discussed, the interpretation of the CFD solver as a discrete time system leads to the conclusion that the identification process is not a function of the adopted time step, as the US is not an approximation of the triangular function. Therefore, the fact that the same results are obtained with such distinct values of time step, as presented in Fig. 11, should actually be the expected outcome. Any small discrepancies between the two sets of results are due to the increased capability of the CFD solver to correctly compute the airflow, with a smaller time step, and never due to a possible difference in the frequency content being resolved by each of those runs, as the frequency content should be absolutely the same in both cases.

The polynomial representations of the aerodynamic transfer functions, that is, the rational function approximations of the data generated by the CFD solver, are obtained with the optimized least-squares calculation described previously. In a case-by-case basis, the number of poles should be determined in order to minimize the error of the approximation polynomial. Using the number of poles $n_\beta = 6$ in Eq. 19, one can observe that a good approximation is obtained, as show in Fig. 12.

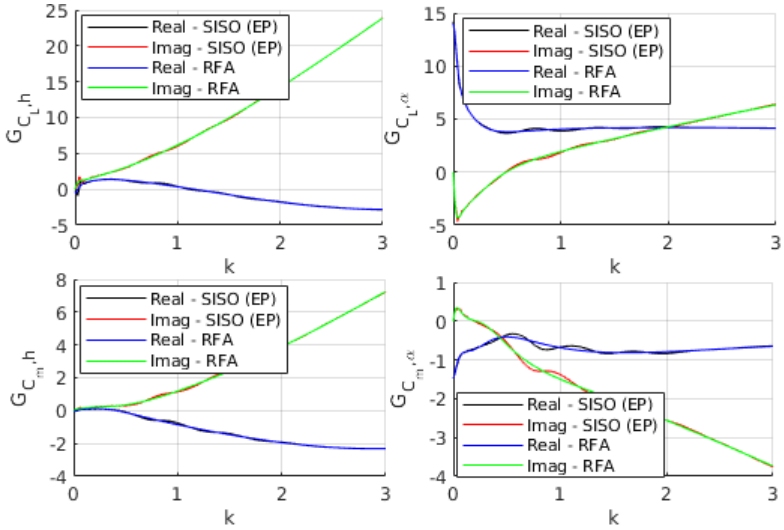

Figure 12. SISO approach aerodynamic transfer function compared with Eversman and Tewari RFA for 6 poles.

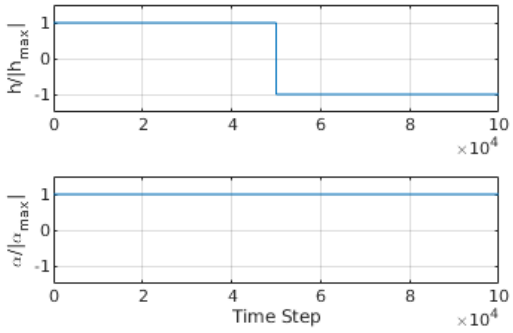

(a) Walsh Functions 1, WF1.

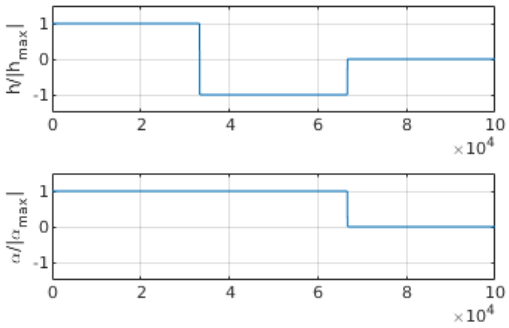

(b) Walsh Functions 2, WF2.

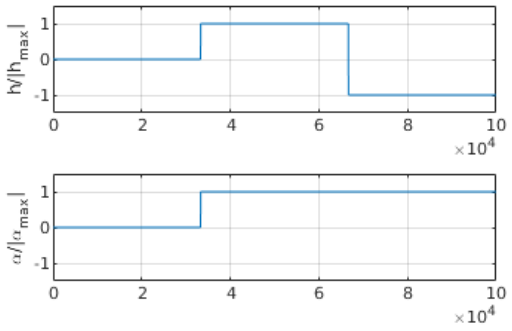

(c) Walsh Functions 3, WF3.

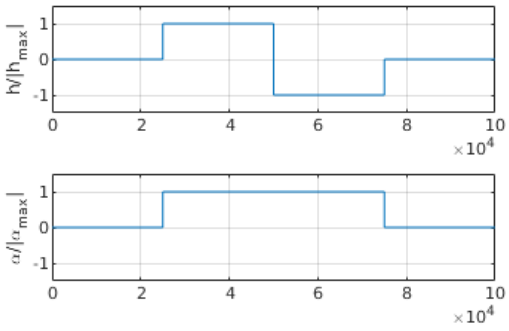

(d) Walsh Functions 4, WF4.

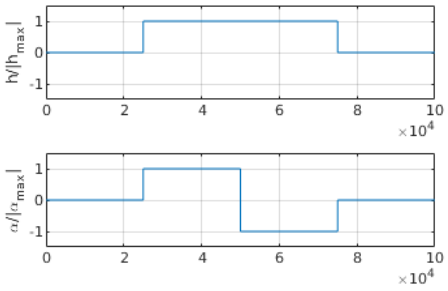

(e) Walsh Functions 5, WF5.

Figure 13. Set of Walsh functions employed by Azevedo (2013).

3.2 Multiple Input–Multiple Output (MIMO) System Identification Techniques

Azevedo (2013) and Azevedo *et al.* (2013) employed the MIMO methodology to obtain the aerodynamic transfer functions of the same aeroelastic system with one single unsteady CFD solution following the work of Raveh (2001), Raveh (2004) and Kim *et al.* (2005) . As in the SISO approach, the excitation functions should excite the complete frequency content of interest, and all degrees of freedom should be excited simultaneously by mutually orthogonal functions. Following Silva (2008), a family of Walsh functions (WF) is used to excite the system due to their similarity to step inputs and, hence, being capable of exciting the whole frequency content. In Azevedo (2013), a set of five Walsh functions, shown in Fig. 13, was employed to obtain the aeroelastic transfer functions.

As previously stated, Azevedo (2013) combined those functions with several parameter settings for the windows employed by the Welch algorithm to obtain the Power Spectral Density (PSD) and Cross-Power Spectral Density (CPSD) functions. There are several possibilities for the windowing parameter settings. Azevedo (2013) investigated the application of the different Walsh functions in combination with some window sizes, obtaining different sets of results that can be classified as satisfactory, labeled here as type A, non-satisfactory and non-oscillatory, labeled type B, and non-satisfactory and oscillatory, labeled here as type C. Figure 14 shows an example of each of those results for the $G_{C_{L,h}}$ aerodynamic transfer function.

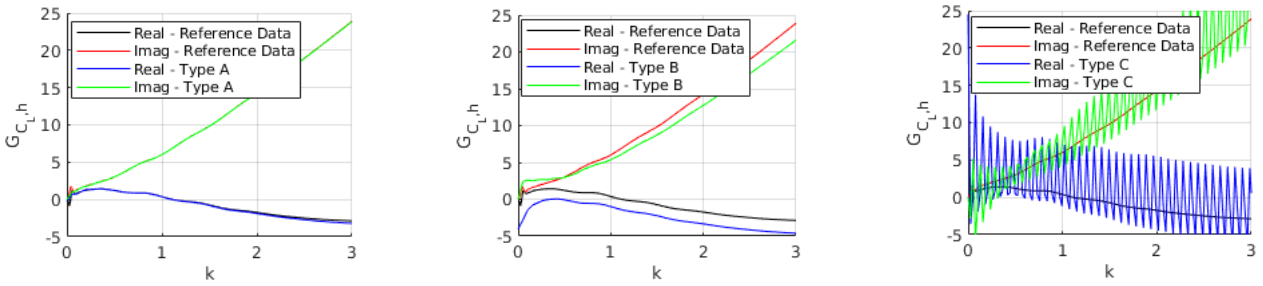

Figure 14. Lift coefficient to plunge excitation transfer functions obtained by Azevedo (2013) compared to Marques and Azevedo (2007).

In order to understand the reason that led to type B results, it should be noted that, for the SISO methodology, the transfer functions obtained from step excitations do not use the actual response of the system as an input to the Fourier transform, but rather the difference between each time step of the response, as shown in Eq. 16. The same applies for the identification process using the MIMO approach with Walsh, or step-like, functions, as indicated in Eq. 17. The PSD and CPSD functions are actually computed over the differences between each time step of the input (α, hl) and output (C_L, C_m) signals of the CFD run. Only for WFs 2, 4 and 5, these difference functions are actually mutually orthogonal, as shown in Table 1. In the work of Azevedo (2013), all the transfer functions of type A were obtained exciting the system with these WFs in which the difference functions are mutually orthogonal. On the other hand, the transfer functions of type B were obtained with non-orthogonal difference Walsh functions. During the investigation of the input settings that

Table 1. Inner product of the inputs for each Walsh function set employed by Azevedo (2013).

Wash Function Set	Inner Product (normalized by 1×10^{-10})
WF1	1
WF2	0
WF3	1
WF4	0
WF5	0

led to the type C results, in which the transfer functions are quite oscillatory, the authors conducted numerical experiments with different types and sizes of windows. In all the experiments that led to an oscillatory solution, the window size of each segment used in the Welch algorithm contained more than one pulse per window, adding to the signal segments a characteristic of a sequence of pulses, or pulse train. Papoulis (1962) shows that the Fourier transform of a pulse train in the time domain, with sampling rate of δt time units, is also a pulse train in the frequency domain, with interval $1/\delta t$. Therefore, the frequency content of the pulse train dominates the Fourier transform of the signal, thus destroying the possibility of appropriately identifying the aerodynamic unsteady response. Therefore, an additional requirement to obtain a good identification is that the widow size used to compute the transfer functions has to be such as to include only one pulse per window.

For completeness, the present work also presents the RFAs obtained following the same approach adopted previously in the SISO analysis, *i.e.*, the use of Eversman and Tewari polynomials of the first type (Eversman and Tewari, 1991)

with 6 aerodynamic states, or 6 poles. Figure 15 presents the aeroelastic transfer functions obtained using the MIMO approach and the RFA interpolations that would allow the creation of the aeroelastic matrix to be used for the forthcoming aeroelastic analysis. One can clearly see in Fig. 15 that the accuracy of the polynomial representations obtained in the present case is equivalent to that shown in Fig. 12, at least in terms of a first inspection. Therefore, if the identification in the MIMO approach is performed in the appropriate manner, results from SISO or MIMO approaches should be equivalent, as already indicated in Azevedo (2013).

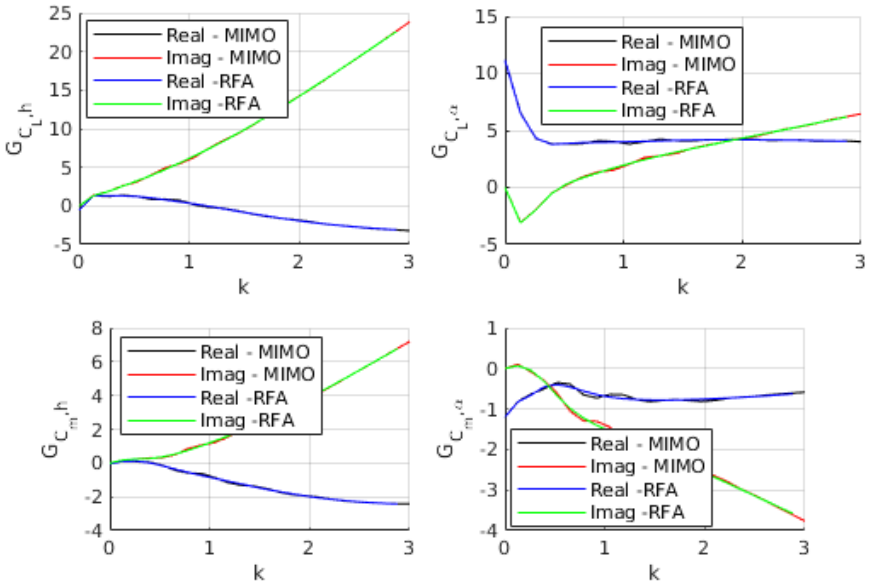

Figure 15. MIMO approach aerodynamic transfer function compared with Eversman and Tewari RFA for 6 poles.

3.3 Flutter Analysis – Root Locus

Although this is not the emphasis of the present work, for the sake of completeness, the root loci of the system stability matrix described in Eq. 21 are presented in Fig. 16 for the two flutter modes obtained by the the present authors using both the SISO and MIMO approaches. The present results are compared with those obtained by Marques and Azevedo (2008b), by direct integration (DI) of the equations of motion. The open blue circles represent the evolution of the aeroelastic eigenvalues obtained with the RFAs, used as the external forces in the aeroelastic equations of motion, obtained using the SISO approach with discrete steps as the system excitation. The predicted flutter characteristic speed presented by Marques and Azevedo (2008b), employing direct integration, is $U^* = 5.48$. In the present work, the characteristic speed obtained with the transfer functions resulting from the SISO approach matched this reference result. However, the flutter characteristic speed obtained using the MIMO approach is $U^* = 6.48$. These results are represented by the open triangular symbols in Fig. 16. The main aspect that can be emphasized from these results is that, although

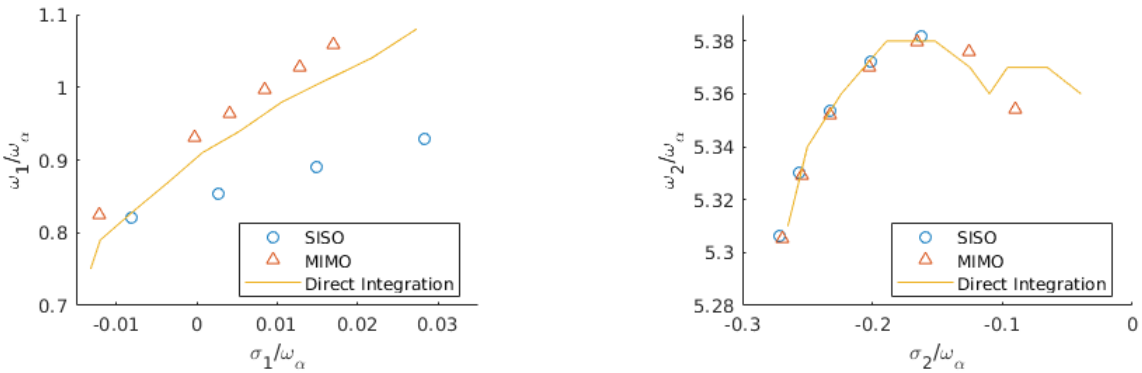

Figure 16. Root Locus for flutter aeroelastic modes 1 and 2.

the aerodynamic transfer functions identified by the SISO and MIMO approaches are very similar to each other, the small differences present in such transfer functions can lead to fairly different polynomial representations. Some preliminary calculations performed in our research group so far have indicated that the optimization process that essentially identifies

the RFAs, which represent the aerodynamic transfer functions in the actual aeroelastic analyses, can be quite sensitive to many numerical parameters associated on how this optimization problem is set up. These aspects are currently being studied and, therefore, they are beyond the intended scope of the present work. Nevertheless, it is clear that additional work is still required in order to achieve the desired robustness in the complete aeroelastic analysis process, even for such a simple canonical test case.

4. CONCLUDING REMARKS

In the present paper, previous work of the research group was revisited with the objective of addressing issues essentially related to the robustness of previous unsteady aerodynamic transfer function predictions. The identification of the aeroelastic transfer functions are performed using both SISO and MIMO approaches and guidelines to solve some of the previously mentioned robustness issues are devised. Regarding the SISO approach, the present authors recommend that the system should be excited using discrete step perturbations in lieu of the exponential pulse or unit sample excitations. The exponential pulse input does not excite the entire frequency content of the system, whereas the unit sample excitation is subject to the limitations of the CFD method to actually solve the time scales involved in the simulation. The present paper also discusses the reasons that led to oscillatory results presented in previous work when applying the MIMO approach. For a successful system identification, the employed Walsh functions used to perturb the system should also be orthogonal on their step incremental values. Additionally, the window sizes employed to compute the power spectral density functions should be such that each window contains only one impulse. Failure to follow such guidelines can lead to inaccurate or oscillatory results.

5. ACKNOWLEDGEMENTS

The authors gratefully acknowledge the support for this research provided by Fundação de Amparo à Pesquisa do Estado de São Paulo, FAPESP, under the Research Grant No. 2013/07375-0. The present work has also received support from Conselho Nacional de Desenvolvimento Científico e Tecnológico, CNPq, under the Research Grant No. 309985/2013-7.

6. REFERENCES

Azevedo, J.H.A., Azevedo, J.L.F. and Silva, R.G., 2012. "Efficient calculation of aerodynamic states for aeroelastic analyses in the frequency domain". *53rd AIAA/ASME/ASCE/AHS/ASC Structures, Structural Dynamics and Materials Conference*. doi:10.2514/6.2012-1716.

Azevedo, J.H.A., Azevedo, J.L.F. and Silva, R.G., 2013. "Effects of the aerodynamic data in a mimo system identification framework for aeroelastic analyses". *54th AIAA/ASME/ASCE/AHS/ASC Structures, Structural Dynamics, and Materials Conference*. doi:10.2514/6.2013-1486.

Azevedo, J.H.A., 2013. *Aeroelastic Studies Using System Identification Techniques*. Master's thesis, Instituto Tecnológico de Aeronáutica, São José dos Campos, Brasil.

Eversman, W. and Tewari, A., 1991. "Consistent rational-function approximation for unsteady aerodynamics". *Journal of Aircraft*, Vol. 28, No. 9, pp. 545–552. doi:10.2514/3.46062.

Harris, F., 1978. "On the use of windows for harmonic analysis with the discrete Fourier transform". *Proceedings of the IEEE*, Vol. 66, pp. 51–83.

Isermann, R. and Munchhof, M., 2009. *Identification of Dynamical Systems*. Springer-Verlag. ISBN 3540788786.

Kim, T., Hong, M., Bhatia, K.G. and SenGupta, G., 2005. "Aeroelastic model reduction for affordable computational fluid dynamics-based flutter analysis". *AIAA Journal*, Vol. 43, No. 12, pp. 2487–2495. doi:10.2514/1.11246.

Lagarias, J.C., Reeds, J.A., Wright, M.H. and Wright, P.E., 1998. "Convergence properties of the Nelder-Mead simplex method in low dimensions". *SIAM J. Optim.*, Vol. 9, No. 1, pp. 112–147.

Marques, A.N. and Azevedo, J.L.F., 2007. "Application of CFD-based unsteady forces for efficient aeroelastic stability analyses". *Journal of Aircraft*, Vol. 44, No. 5, pp. 1499–1512. doi:10.2514/1.27510.

Marques, A.N. and Azevedo, J.L.F., 2008a. "Numerical calculation of impulsive and indicial aerodynamic responses using computational aerodynamics techniques". *Journal of Aircraft*, Vol. 45, No. 4, pp. 1112–1135. doi:10.2514/1.32151.

Marques, A.N. and Azevedo, J.L.F., 2008b. "A z-transform discrete-time state-space formulation for aeroelastic stability analysis". *Journal of Aircraft*, Vol. 45, No. 5, pp. 1564–1578. doi:10.2514/1.32561.

Oliveira, L.C., 1993. *Uma Metodologia de Análise Aeroelástica com Variáveis de Estado Utilizando Técnicas de Aerodinâmica Computacional*. Master's thesis, Instituto Tecnológico de Aeronáutica, São José dos Campos, Brasil.

Papoulis, A., 1962. *The Fourier Integral and its Applications*. McGraw-Hill, New York.

Rausch, R.D., Batina, J.T. and Yang, H.T.Y., 1990. "Euler flutter analysis of airfoils using unstructured dynamic meshes". *Journal of Aircraft*, Vol. 27, No. 5, pp. 436–443. doi:10.2514/3.25295.

Raveh, D.E., 2001. "Reduced-order models for nonlinear unsteady aerodynamics". *AIAA Journal*, Vol. 39, No. 8, pp. 1417–1429. doi:10.2514/2.1473.

Raveh, D.E., 2004. "Identification of computational-fluid-dynamics based unsteady aerodynamic models for aeroelastic analysis". *Journal of Aircraft*, Vol. 41, No. 3, pp. 620–632. doi:10.2514/1.3149.

Silva, W.A., 1997. "Identification of linear and nonlinear aerodynamic impulse responses using digital filter techniques". *NASA TM-112872*.

Silva, W.A., 2008. "Simultaneous excitation of multiple-input/multiple-output CFD-based unsteady aerodynamic systems". *Journal of Aircraft*, Vol. 45, No. 4, pp. 1267–1274. doi:10.2514/1.34328.

Vepa, R., 1977. *Finite State Modeling of Aeroelastic Systems*. Stanford University. Stanford. CA.

Welch, P., 1967. "The use of fast Fourier transform for the estimation of power spectra: A method based on time averaging over short, modified periodograms". *IEEE Transactions on Audio and Electroacoustics*, Vol. 15, No. 2, pp. 70–73. doi:10.1109/TAU.1967.1161901.

7. RESPONSIBILITY NOTICE

The authors are solely responsible for the printed material included in this paper.